Supporting Information

Superior capacitive performances achieved in wide HOMO-LUMO gap cyanoethyl cellulose nanocomposites via forming built-in electric field

Zhicheng Li[a,1], Yu Zhang[c,1], Zhongbin Pan[a,*], Xu Fan[a], Hao Wang[a], Peng Li[b], Haiming Huang[c,*], Weiliang Wang[d], Jinjun Liu[a], and Jiwei Zhai[e,*]

[a]School of Materials Science and Chemical Engineering, Ningbo University, Ningbo, Zhejiang, 315211, China. E-mail: panzhongbin@163.com (Zhongbin Pan).

[b]School of Materials Science and Engineering, Liaocheng University, Liaocheng, 252059, China.

[c]Solid State Physics & Material Research Laboratory, School of Physics and Materials Science, Guangzhou University, Guangzhou 510006, China. E-mail: huanghm@gzhu.edu.cn (Haiming Huang).

[d]School of Physics, Guangdong Province Key Laboratory of Display Material and Technology, Sun Yat-sen University, Guangzhou 510275, China.

[e]School of Materials Science & Engineering, Tongji University, 4800 Caoan Road, Shanghai, 201804, China. E-mail: apzhai@tongji.edu.cn (Jiwei Zhai).

Experimental

Fabrication of BFO/CRC and BFO@AO/CRC composite films

The solution casting was employed to fabricate nanocomposite films. BFO and BFO@AO nanofibers with different proportions were adequately dispersed in DMF, and then CRC matrix was incorporated in the above solution and mixed until homogeneous. All solutions were placed in a vacuum environment to eliminate internal air, then cast onto ITO glass.

Characterization

Characterization was carried out using a field emission Scanning Electron Microscope (FE-SEM, SU8020, JEOL, Tokyo, Japan) to obtain the SEM images of $BiFeO_3$ nanofibers. Transmission Electron Microscopy (TEM, JEM-2100, JEOL Ltd., Tokyo, Japan) was used to obtain the morphology of $BiFeO_3$@Al_2O_3 nanofibers. The crystal structure of the composite materials was obtained by X-Ray Diffraction (XRD) on a D8 Advance X-ray diffractometer. The dielectric properties of all samples at room temperature and different temperatures were measured by an LCR (TH 2838A, Changzhou Tonghui Electronics Co., Ltd., China) in the range of 10^3 to 10^6 Hz. The polarization-electric field (*P*-*E*) loops were measured by the Premier II Ferroelectric test system (Poly *K*). The Young's modulus values were derived from strain-stress curves measured with a TA RSA-G2 Solids Analyzer, using a constant linear stretching rate of 10 mm/min The fast discharge tests were performed using a CF-003 test system (Instruments Technology, China).

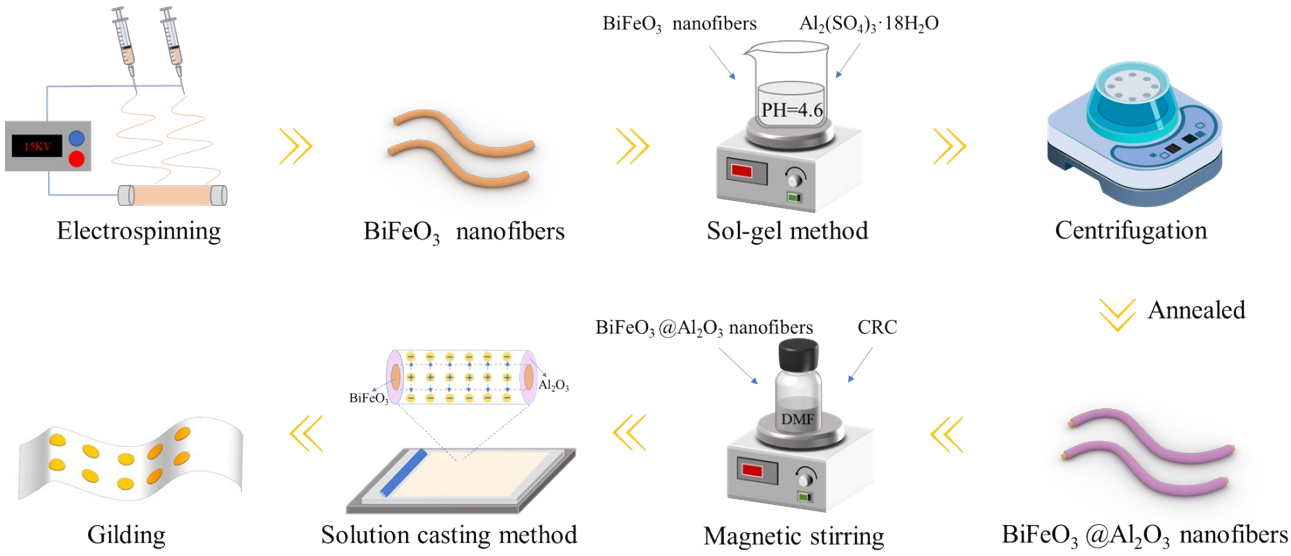

Figure S1. The preparation process of BFO@AO/CRC composite films.

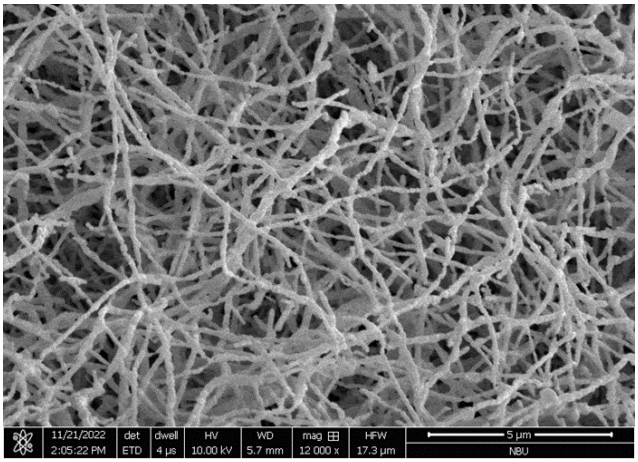

Figure S2. The SEM image of BFO nanofibers.

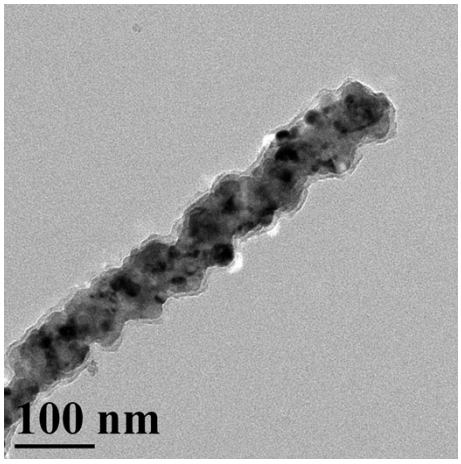

Figure S3. The TEM image of BFO@AO nanofibers.

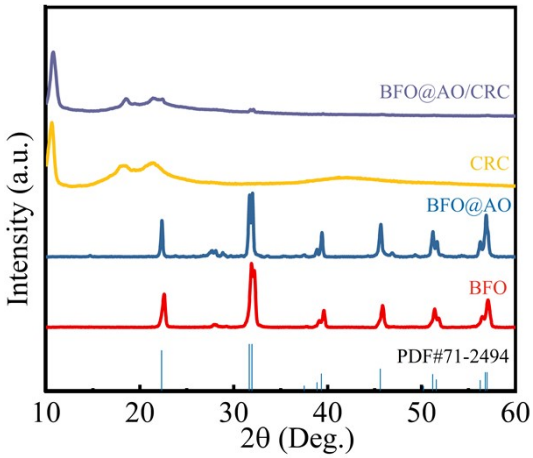

Figure S4. The XRD pattern of BFO, BFO@AO, CRC, and BFO@AO/CRC.

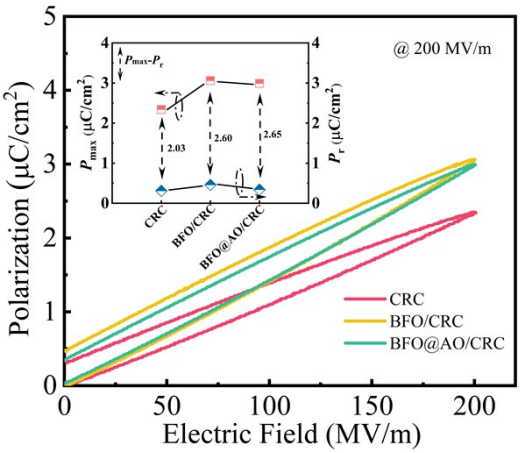

Figure S5. The *P-E* curves of CRC, BFO/CRC, BFO@AO/CRC films at 200 MV/m. (inset: The P_{max} and P_r of CRC, BFO/CRC, BFO@AO/CRC films at 200 MV/m)

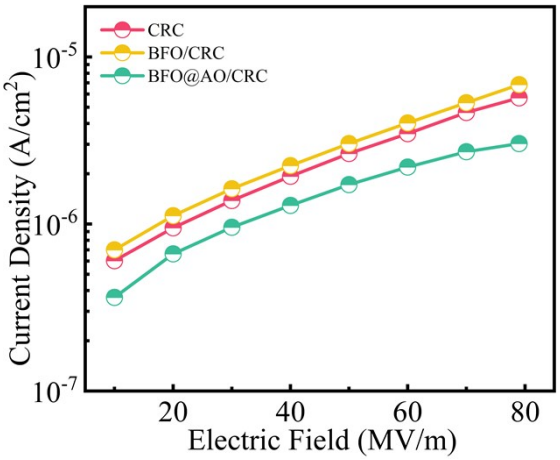

Figure S6 The leakage current density of CRC, BFO/CRC, BFO@AO/CRC films.

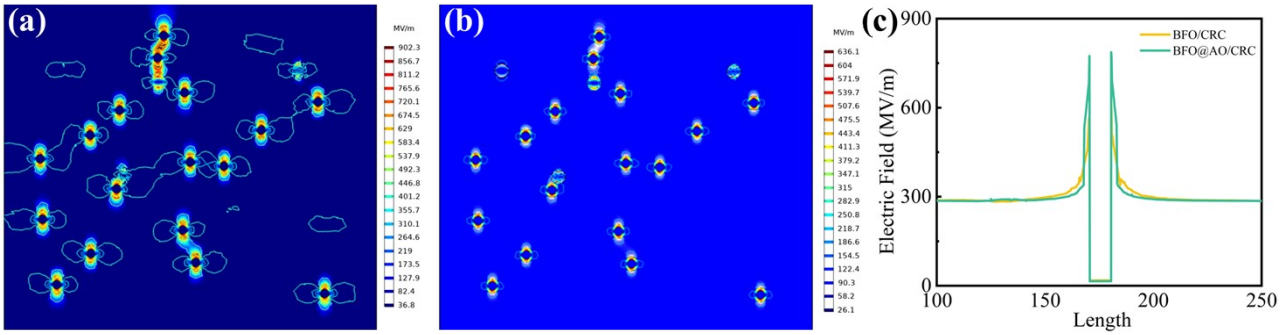

Figure S7. Finite element simulation on electric field distribution of (a) BFO/CRC and (b) BFO@AO/CRC cross-section of dielectric film. (c) The comparison of breakdown strength values simulated by computer with BFO/CRC and BFO@AO/CRC composite.

We set up a cuboid (400×500×300), and several nanofibers were randomly parallel distributed inside the cuboid. We select a cross-section to analyze the electric field distortion and then make a potential line pass perpendicularly through the nanofiller to calculate the electric field strength.

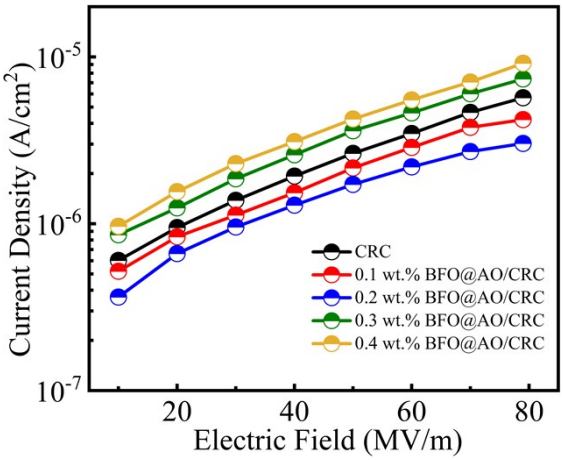

Figure S8. The leakage current density of CRC and its nanocomposites with different content of BFO@AO.

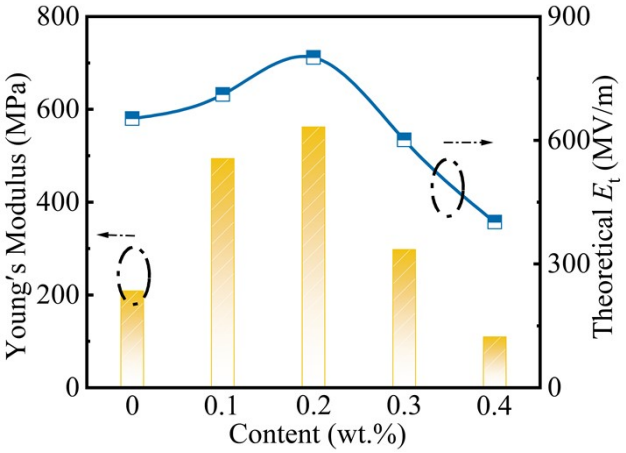

Figure S9. Young's modulus and theoretical E_t of CRC and its nanocomposites with different content of BFO@AO.